Vapor Phase Transport Deposition, Characterization, and Applications of Large Nanographenes

Ahmad N. Abbas [‡,¶], *Bilu Liu* [‡], *Akimitsu Narita* [ϒ], *Lukas F. Dössel* [ϒ], *Bo Yang* [ϒ], *Wen Zhang* [ϒ], *Jianshi Tang*[†], *Kang L. Wang*[†], *Hans Joachim Räder* [ϒ], *Xinliang Feng* [ϒ], *Klaus Müllen* [ϒ] *and Chongwu Zhou* [‡*]

‡ Department of Electrical Engineering, University of Southern California, Los Angeles, California 90089, United States

ϒ Max Planck Institute of Polymer Research, Ackermannweg 10, 55128 Mainz, Germany

† Device Research Laboratory, Department of Electrical Engineering, University of California, Los Angeles, California, 90095, USA

¶ Department of Electrical Engineering, University of Jeddah, Abdullah Sulayman St, Jeddah 22254, Saudi Arabia

* Email: chongwuz@usc.edu

Supporting Information

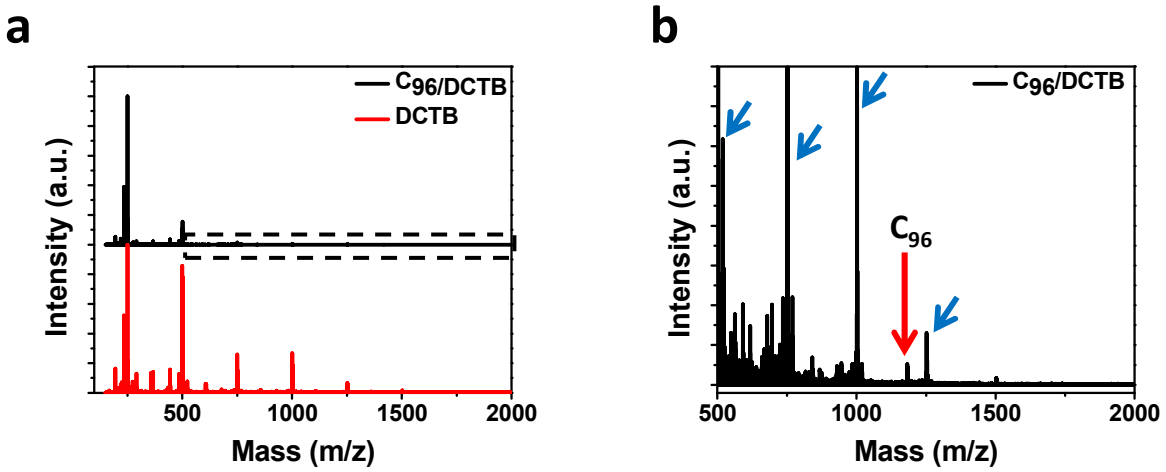

Figure S1. MALDI-TOF MS characterization of C_{96} films deposited *via* VPT a) MALDI-TOF MS spectra of C_{96}/DCTB (black) and DCTB matrix (red) for a wider mass range. b) Zoom in image in the dashed area of (a), which shows a peak from C_{96} (red arrow) that doesn't appear in the spectrum of only DCTB, confirming the sublimation of undamaged C_{96}. All the other signals can be assigned to the clusters of DCTB matrix (blue arrows) and their fragments. The signals at m/z = 250, 500, 750 1000, 1250, and 1500 are obviously the peaks of DCTB clusters, because the molecular weight of DCTB is 250 Da. The other peaks, especially in the mass range of 500–750 Da and 750–1000 Da, could be attributed to the recombination of fragment ions with DCTB matrix clusters.

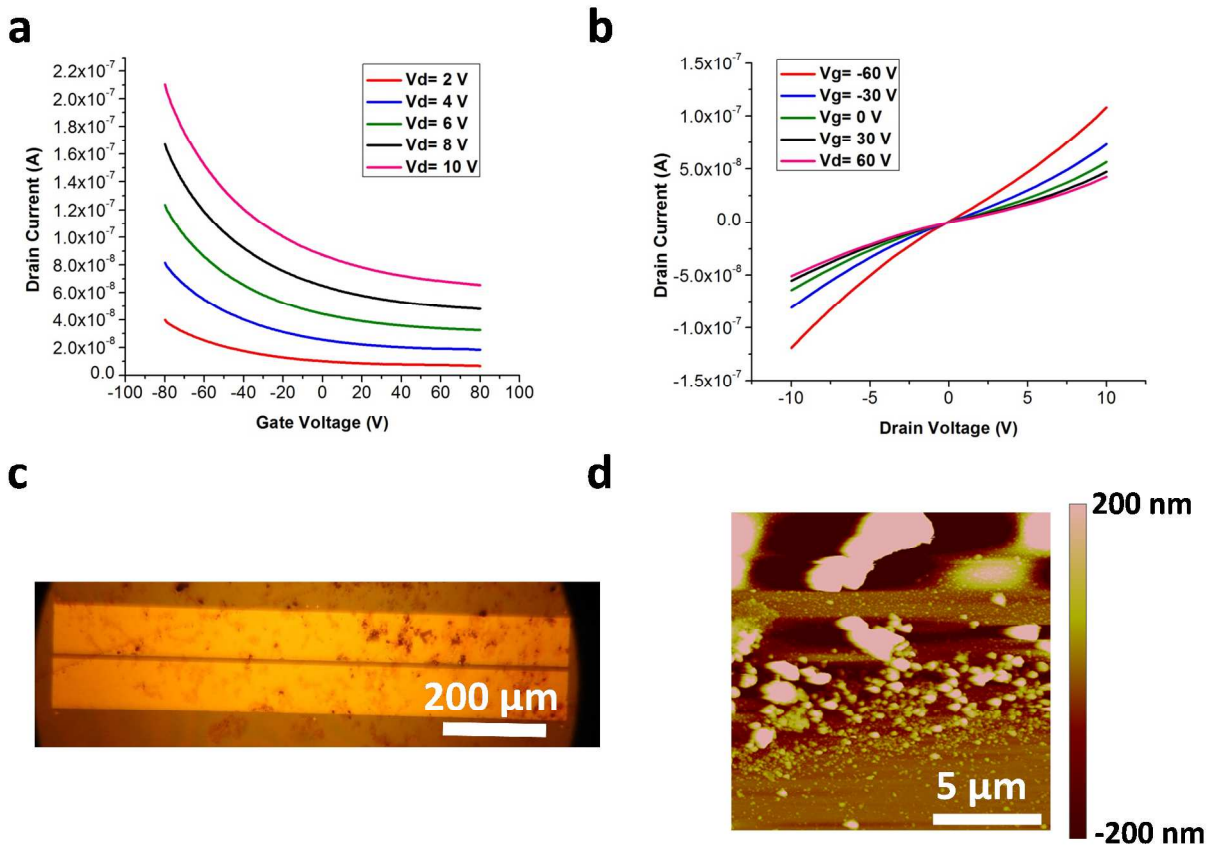

Figure S2. Electrical measurements of liquid-phase dispersed GNP TFT. a) I_d-V_g characteristics of a liquid-phase dispersed GNP TFT on P^{++} Si/ 300 nm SiO_2 with Ti/Au electrodes at different drain biases showing a non-depletable FET with a current on/off ratio of ~ 2-3. b) I_d-V_d characteristics of the liquid-phase processed GNP FET at different gate voltages. c) Optical image of a liquid-phase dispersed GNP TFT showing visible aggregates. d) AFM image of a liquid-phase dispersed GNP revealing large particles and RMS roughness of ~ 10 – 250 nm.

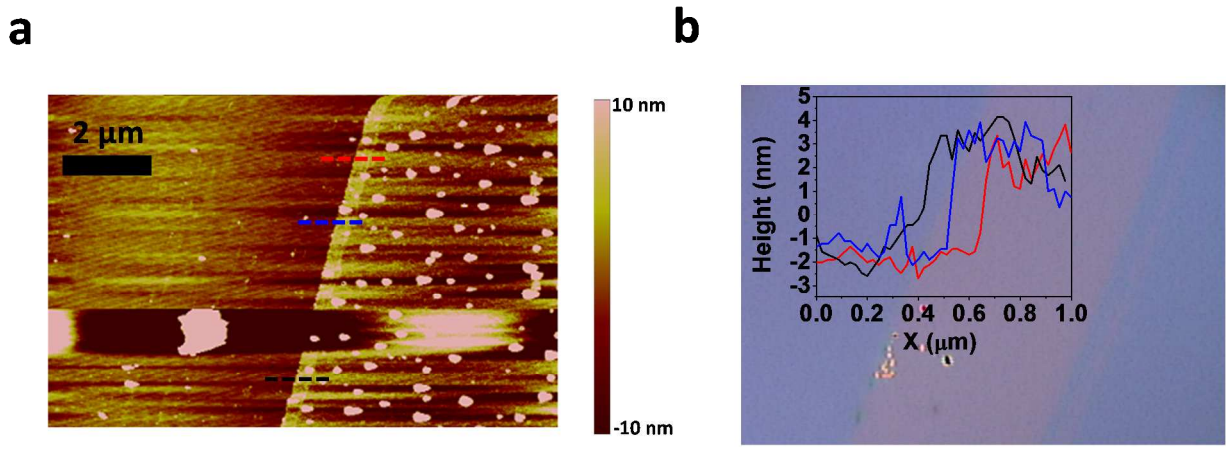

Figure S3. AFM characterization of GNP thin-film thickness. a) AFM height image of a Si/SiO_2 substrate after GNP deposition scratched gently with a micro probe to expose the substrate and analyze the height profile. The three dashed lines correspond to the height profile taken at different positions. b) An optical image of the substrate in (a) revealing an optical contrast in the probe scratched area. Inset shows the three height profiles taken at positions marked in (a) with heights of ~ 5.3 nm (black), 4.8 nm (blue), and 2.9 nm (red).

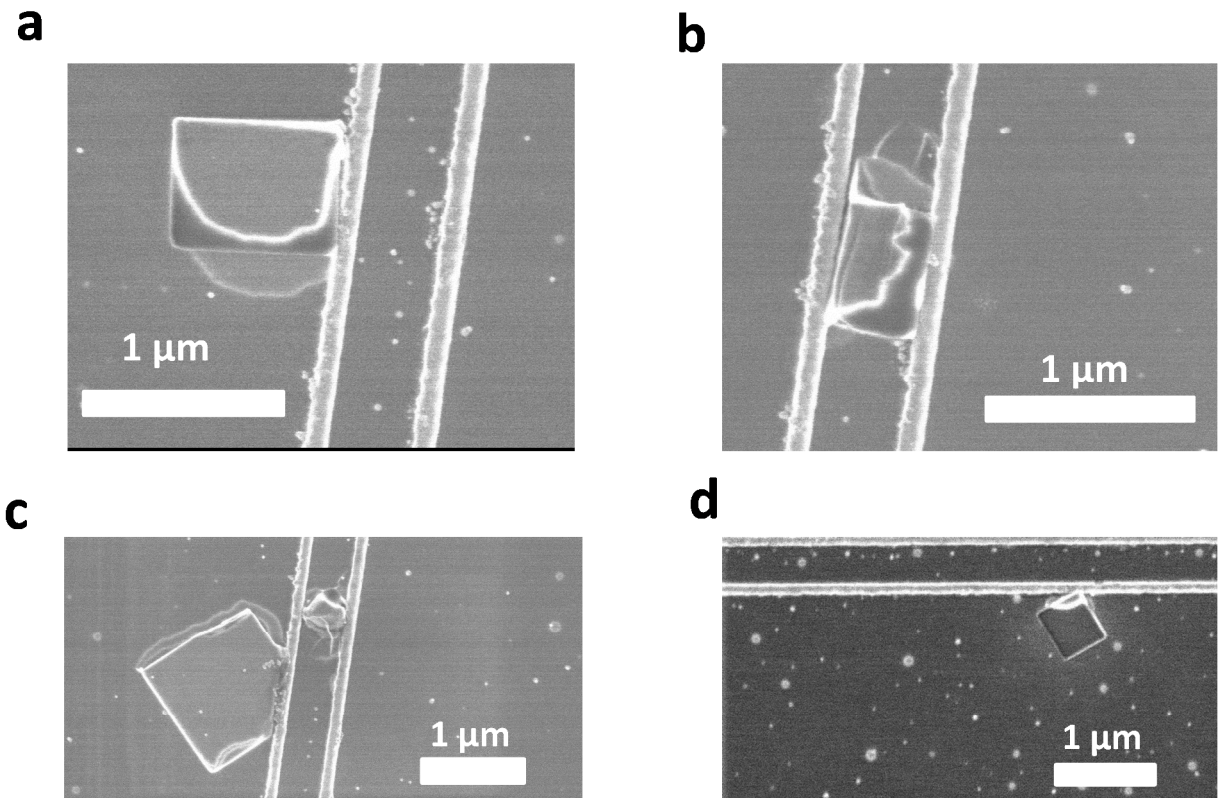

Figure S4. a- d) SEM images of GNP crystals formed on Ti/Au electrode.

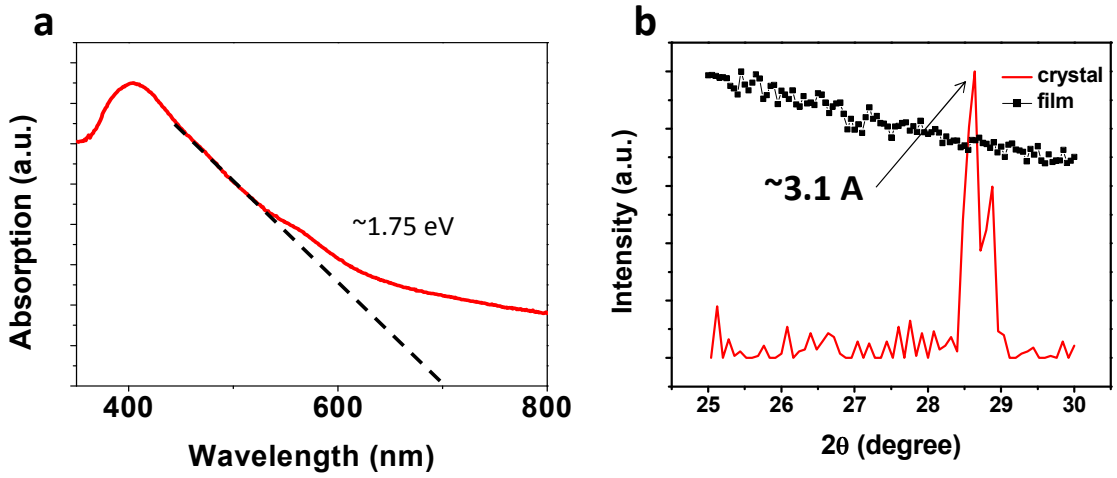

Figure S5. a) UV-Vis absorption spectrum of GNP dispersed in THF. The optical bandgap of the GNP can be extrapolated from the x-intercept yielding a value of ~1.75 eV. b) X-ray diffraction (XRD) spectrum of a sample with GNP crystals (red) and a flat GNP film (black) indicating an ordered assembly of GNP in the case of crystals. The XRD peak in the crystal sample corresponds to a crystal constant of ~3.1 A.

	G-band FWHM	D-band FWHM	G-band position (cm^{-1})	D-band position (cm^{-1})
Solution GNPs	27	52	1602	~1332
Sublimated GNPs	76	208	1602	~1360
Solution C_{96}	22	54	1608	~1315
Sublimated C_{96}	27	60	1605	~1319

Table S1. Analysis of Raman spectral peaks of liquid-phase-processed and sublimated GNPs/C_{96}. In the above table, the full-width at half-maximum (FWHM), G and D band positions of different samples are listed. It can be seen that for GNPs, the FWHM is different for liquid-phase-processed and sublimated samples, while the FWHM is the same for liquid-phase-processed and sublimated C_{96}. This is due to the removal of dodecyl side chains in the case of sublimated GNPs.

Section S1. Discussion of the optical properties of graphene nanopatches (GNPs):

The prospect of using nanographenes in various applications relies heavily on the processing of these molecules into various forms (e.g. films) and the applicability of such forms. An important prospect of using GNPs is in the field of optoelectronics and photonics due to their adjustable lengths and edge structures which directly modify the optical properties of this material. [1-3] Accordingly, the optical characterization of the sublimated GNP films is very important for the development of novel optical devices utilizing these films. In order to characterize the intrinsic optical properties of GNP, photoluminescence (PL) measurements of GNP were carried out in a dispersion in 1,2-di*chlorobenzene (D*CB), where the interaction between dispersed GNPs is minimized. Fig S7a shows a typical PL spectrum of GNP dispersion under a 300 nm excitation wavelength. As it can be seen, the fluorescence (*i.e.* PL) of GNPs when exciting the dispersion with a 300 nm source reveal two peaks at ~350 nm and 666 nm while the absorption spectrum of such dispersion shows a peak at 300 nm and another broad peak at 410 nm. To investigate the radiative nature of absorption, we measured the excitation response of PL peaks at 350 nm and 666 nm. Fig S7b shows the fluorescence intensity at 666 nm (black) and 350 nm (red) as a function of excitation wavelength revealing a peak around ~ 299 nm where the absorption of the material mostly leads to a radiative deactivation. On the other hand, by observing both PL excitation and absorption spectra, we conclude that GNP absorption for wavelengths >350 nm, including the peak at 410 nm, mostly comprise of nonradiative deactivation processes. In order to assess the applicability of sublimated GNP films in optoelectronic and photonic applications, the fluorescence of films of thickness between ~ 2 to 5 nm must not be quenched by nonradiative scattering mechanisms induced by the substrate and interaction between GNPs. This PL quenching has been observed in other nanomaterials such as

carbon nanotubes (CNTs). [4-6] To study such issues, transient photoluminescence (TPL) measurements were carried out to compare the fluorescence lifetimes of GNP dispersions and GNP films. Due to the limited available choices for laser wavelengths, we chose a laser excitation wavelength of 400 nm and a PL emission at 450 nm (Fig S6). Fig S7c shows TPL measurement of GNP dispersion and a GNP film for emission at 450 nm. Table 1 summarizes the TPL fitting parameters, including carrier lifetimes, for both films and dispersions. For GNP dispersion, the longest carrier lifetime is 9.1 ns and it represents the majority of the radiative population (*i.e.* 58 %). On the other hand, the longest carrier lifetime for GNP films is 4.3 ns and it represents only ~20% of the total radiative processes. The difference in the main radiative component carrier lifetime between the dispersion and the films is due to different GNP interaction mechanisms. The variation in GNP/GNP interaction, GNP/solvent interaction and GNP/substrate interaction in the case of GNP films compared to dispersions lead to a slight alteration of the electronic properties of GNPs and their carrier lifetimes. Moreover, the increase in the percentage of short lived species from GNP dispersion to films can be explained by surface polar scattering mechanisms due to the substrate effect and other scattering mechanisms induced by GNP/GNP junctions. Additionally, due to the inability to sublimate GNP species with the largest molecular weight, the distribution of species in the GNP dispersion and GNP films is different, and this lead to three different lifetimes in GNP dispersion compared to only two in the GNP film.

Table 1. Carrier lifetimes for GNP films and dispersions extracted from fitting parameters using fractional intensities of positive decay components.

Carrier lifetimes	GNP dispersion	GNP film
τ_1	9.1 ns (57.62 %)	4.3 ns (20.19%)
τ_2	2 ns (33.57%)	1 ns (79.81%)
τ_3	0.3 ns (8.81 %)	

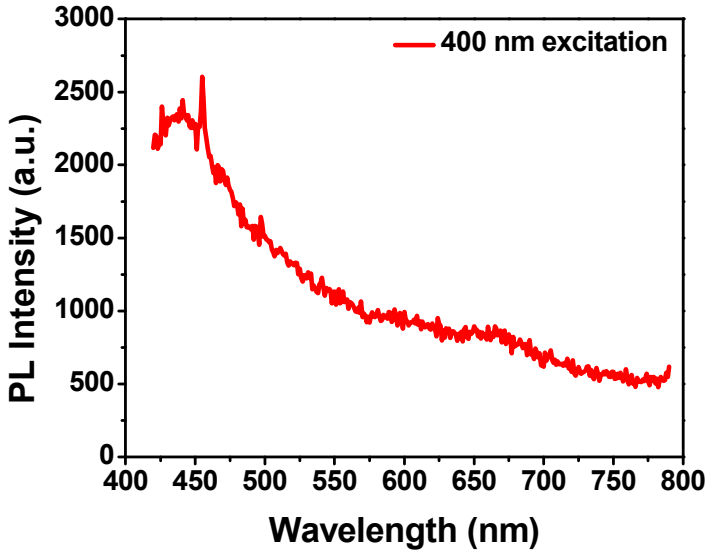

Figure S6. Steady-state PL spectrum of GNP dispersed in DCB showing a PL peak around 450 nm when exciting the sample with a 400 nm source.

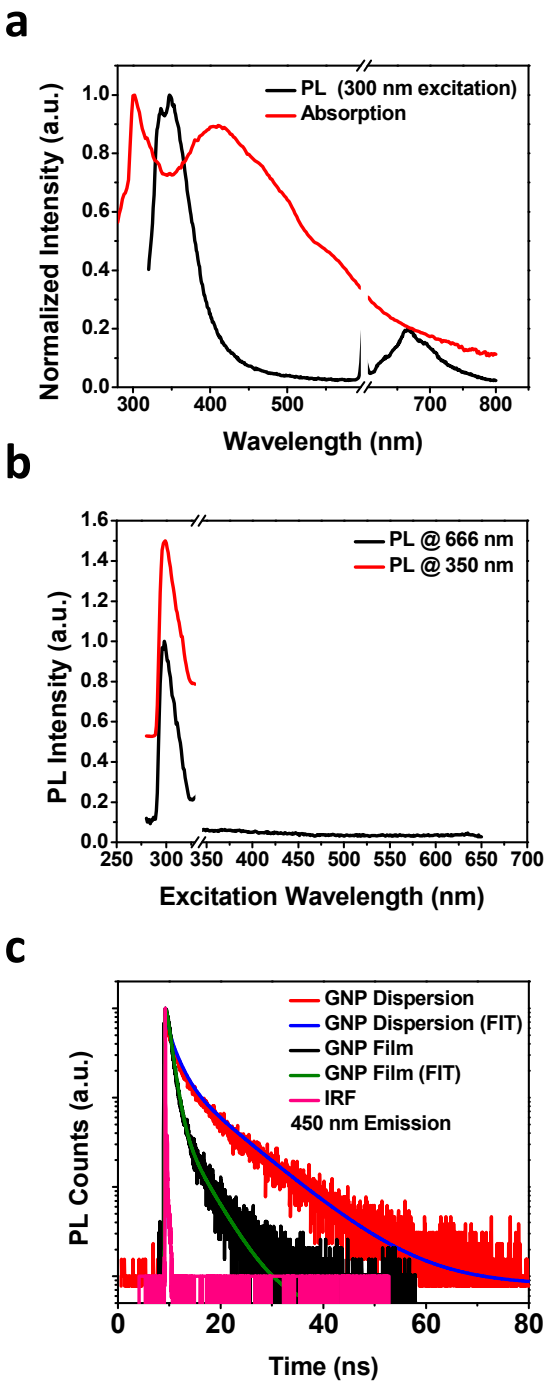

Figure S7. Investigations of the optical properties of the sublimated GNP dispersion and films. a) Steady-state PL spectrum of GNP dispersed in DCB (black) showing a clear PL peak around 350 nm and 666 nm when exciting the sample with a 300 nm source and the corresponding UV/vis

absorption spectrum of GNP dispersed in DCB (red) showing peaks at ~300 nm and 410 nm. The x-axis is broken at the position of the peak of twice the excitation wavelength (*i.e.* 600 nm) b) PL excitation spectrum with emission fixed at 666 nm (black) and 350 nm (red) for GNP dispersed in DCB as a function of source wavelength. Maximum PL response corresponds to excitation at ~299 nm which agrees with the absorption peak indicating radiative deactivation processes at such wavelength. The x-axis is broken at the position of the peak of half the PL wavelength (*i.e.* 333 nm) c) Normalized transient PL measurements of emission at 450 nm for both GNP dispersed in DCB (red) and sublimated GNP film on P^{++} Si/ 300 nm SiO_2 (black) when exciting the samples with a 400 nm laser. Moreover, the fittings for both GNP dispersion and film TPL measurements are shown in blue and green, respectively. Additionally, the instrument response function (IRF) is plotted in pink with 22ps time resolution. The average intensity-weighted carrier lifetimes for GNP solution and sublimated films are 5.913 ns and 1.636 ns respectively.

Methods:

- **TPL:** Transient PL measurements were carried out using an excitation wavelength of 400 nm obtained from the second harmonic generation of the fundamental 800 nm laser (250 kHz Ti:sapphire amplifier, Coherent RegA 9050). The emission was collected at 450 nm using a R3809U-50 Hamamatsu PMT with a Becker and Hickl SPC 630 detection module (22 ps time resolution).

References:

1. Mueller, M. L.; Yan, X.; McGuire, J. A.; Li, L.-s., Triplet States and Electronic Relaxation in Photoexcited Graphene Quantum Dots. *Nano Letters* ***10***, 2679-2682 (2010).

2. Zhu, S.; Wang, L.; Li, B.; Song, Y.; Zhao, X.; Zhang, G.; Zhang, S.; Lu, S.; Zhang, J.; Wang, H.; Sun, H.; Yang, B., Investigation of photoluminescence mechanism of graphene quantum dots and evaluation of their assembly into polymer dots. *Carbon* **77**, 462-472 (2014).

3. Englert, J. M.; Hauke, F.; Feng, X.; Mullen, K.; Hirsch, A., Exfoliation of hexa-peri-hexabenzocoronene in water. *Chemical Communications* ***46***, 9194-9196 (2010).

4. Lefebvre, J.; Homma, Y.; Finnie, P., Bright Band Gap Photoluminescence from Unprocessed Single-Walled Carbon Nanotubes. *Physical Review Letters* **90**, 217401 (2003).

5. Lefebvre, J.; Austing, D. G.; Bond, J.; Finnie, P., Photoluminescence Imaging of Suspended Single-Walled Carbon Nanotubes. *Nano Letters* **6**, 1603-1608 (2006).

6. O'Connell, M. J.; Bachilo, S. M.; Huffman, C. B.; Moore, V. C.; Strano, M. S.; Haroz, E. H.; Rialon, K. L.; Boul, P. J.; Noon, W. H.; Kittrell, C.; Ma, J.; Hauge, R. H.; Weisman, R. B.; Smalley, R. E., Band Gap Fluorescence from Individual Single-Walled Carbon Nanotubes. *Science* **297,** 593-596 (2002).